

# Renewable Bis-benzoxazine Monomers from Lignin Derivatives: Synthesis, Characterization and Studies on Curing Behavior

CHUNYAN LIU\*, YUNHE LIU, ZIHAN PAN, QIUTING LI, HAN XU  
AND TAO LIU

*Chengde Petroleum College, Department of Chemical Engineering,  
Chengde 067000, Hebei, China*

## ABSTRACT

*In this work, a series of novel lignin-based bis-benzoxazine monomers were efficiently synthesized by the reaction of renewable phenols: guaiacol, vanillyl alcohol, eugenol, vanillin with ethylene diamine and paraformaldehyde. The chemical structures of these lignin-based bis-benzoxazine monomers were confirmed by <sup>1</sup>H-NMR, <sup>13</sup>C-NMR and FTIR, indicating the formation of benzoxazine ring. The obtained bis-benzoxazine monomers were cured via thermal treatment. The curing behavior of these lignin-based bis-benzoxazine monomers were compared and analyzed via differential scanning calorimetry (DSC), showing that Va-e possessed higher ring-opening polymerization activity than G-e, while E-e and V-e had lower curing activity than G-e.*

*KEYWORDS: Lignin-based, Bis-benzoxazine, Curing kinetics, Thermal stability.*

## 1. INTRODUCTION

Benzoxazine resin, as a special kind of thermoset phenolic resin, can be prepared by the Mannich condensation reaction of phenol, amine and paraformaldehyde<sup>[1-3]</sup>. Meanwhile the corresponding polymer, polybenzoxazine can be obtained by the ring-opening polymerization

of benzoxazine ring under heat treatment<sup>[4-6]</sup>. In addition to having the typical performances of traditional phenolic resins, polybenzoxazines also possess some unique features over traditional phenolic resins, which include high thermal stability, no need of catalyst, near-zero curing shrinkage, good mechanical properties,

high glass transition temperature ( $T_g$ ), lower flammability, low water absorption and dielectric. As such, benzoxazine resins were extensively used in the field of aviation, electronics, and composites<sup>[7,8]</sup>.

The utilization of renewable raw materials to replace petroleum-based ones for producing pre-polymers or resins, not only prevents the environmental pollution from the petroleum-based plastics, but also saves the limited fossil resource<sup>[9,11]</sup>.

Lignin, as the main components of lignocellulose, which accounts for 15%-30% of wood composition, is the second major natural organic compounds in nature. Lignin is usually a by-product of the pulp and paper industry. And the majority of raw material is burned as energy, although it has many other added-value utilizations<sup>[12-14]</sup>. The direct application of lignin in polymer synthesis is limited because of the complexity of its structure<sup>[15]</sup>. However, a large number of resins, including phenolic resin, polyester, benzoxazine resin, epoxy resin and polyurethane, have been prepared by functionalization hydroxyl groups of lignin<sup>[16-18]</sup>.

With the continuous development of controlled degradation of lignin, a large number of lignin derivatives phenols were obtained. These lignin derivatives include eugenol, vanillin, guaiacol, vanillyl alcohol and so on. These bio-based monomers are suitable candidate for the synthesis of various polymer materials, since they avoid the competition with food resources perfectly<sup>[19-21]</sup>. In recent years, series of bio-based benzoxazine resins derived from modified lignin and lignin derivative monomers (vanillin, guaiacol, eugenol) have been reported. For example, Ghizelle Jane Abarro et al.

synthesized a kind of polybenzoxazine based on phenolated organosolv lignin with good thermal stability and flame retardancy<sup>[22]</sup>. Ganesh A. Phalakpoly et al. synthesized several kinds of benzoxazine-urethane coating from guaiacol, and these coatings showed excellent corrosion resistance<sup>[23]</sup>. P. Thirukumaran et al. reported the preparation of a series of allyl-containing bio-based benzoxazine monomer from eugenol, various aromatic diamines, and paraformaldehyde. The corresponding polybenzoxazine showed adjustable thermodynamic performance<sup>[24]</sup>. Indra K. Varma et al. reported the synthesis and polymerization of lignin-based bifunctional benzoxazines obtained from different diamines and vanillin. Comparison with commercial benzoxazine, the incorporation of vanillin in the structure of benzoxazine resulted in higher crosslinking density and better thermal stability<sup>[25]</sup>.

However, no one has ever discussed the effect of different substituents of these lignin-based bis-benzoxazine monomers on the curing behavior and thermal stability of corresponding polybenzoxazines. In this study, we select renewable raw materials guaiacol, vanillyl alcohol, eugenol and vanillin as starting materials to prepare a series of lignin-based bis-benzoxazine monomers. And the structure features and curing behaviors of all these bis-benzoxazine monomers as well as the thermal stability of corresponding polybenzoxazines were all investigated in detail.

## EXPERIMENTAL

### Raw materials

Guaiacol, vanillyl alcohol, eugenol, vanillin, 1, 4-dioxane, ethylene diamine, chloroform, magnesium sulfate, paraformaldehyde, and sodium hydroxide were bought

from Sinopharm Chemical Reagent Co., Ltd. All chemicals were used as received without any purification.

### Measurements

Fourier Transform Infrared spectra (FTIR) of the bio-based monomers were recorded on an FTIR spectrometer (Perkin Elmer FTIR C91158, UK) in absorbance mode. The samples were mixed with spectroscopy-grade KBr powder and then be compressed into pellet. The spectra were recorded in the range of 400 to 4000 $\text{cm}^{-1}$  with 4 $\text{cm}^{-1}$  resolution. 32 scans were collected for each sample to ensure accuracy of the final testing results.

The proton  $^1\text{H}$  and carbon  $^{13}\text{C}$ NMR spectra of the bio-based monomers were both recorded with an Avance III Bruker 400MHz NMR spectrometer (Bruker, Switzerland) at room temperature. Tetramethylsilane (TMS) and  $\text{CDCl}_3$  were used as the internal standard and solvent, respectively. The signals of sample were averaged from 16 transients for  $^1\text{H}$  NMR and 300 transients for  $^{13}\text{C}$  NMR to yield spectra with sufficient signal-to-noise ratio.

The curing behavior of the bio-based monomers was studied by differential scanning calorimetric (DSC) on a TA Instruments DSC model 2920 (TA, USA). Approximate 10mg sample was crimped in an aluminum crucible. The high purity nitrogen was used as the protection atmosphere with the flow rate of 50 ml/min.

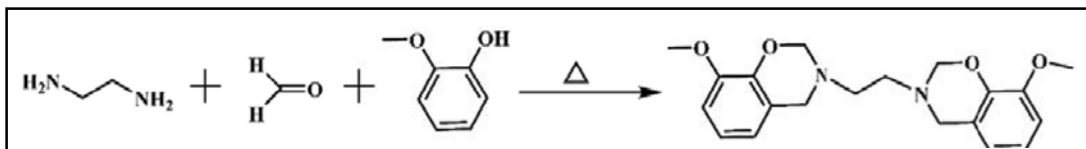
The viscosity was measured by a Bohlin Gemini 200 Rheometer in steady shear mode with a heating rate of

3 $^\circ\text{C}$  /min and an angular frequency of 1Hz. The experiments were performed at 200 $^\circ\text{C}$  and under a nitrogen atmosphere.

Thermogravimetric analysis (TGA) was used to investigate the thermal stability of the bio-based polybenzoxazine resins and the measurements were carried out on a Perkin Elmer TA 2100-SDT 2960 (Perkin Elmer Instruments) in a temperature range of 50 to 800 $^\circ\text{C}$  and a heating rate of 10 $^\circ\text{C}$ /min under nitrogen at a flow rate of 20 mL/min.

### Synthesis of guaiacol-based bis-benzoxazine precursor: G-e

19.9 g guaiacol (0.16 mol), 4.8 g ethylenediamine (0.08 mol), 12.1 g paraformaldehyde (0.40 mol, 5.0 equiv.) and 150 mL 1,4-dioxane were introduced into a round-bottom 250 mL glass flask equipped with a nitrogen inlet, a condenser and a magnetic stirrer. Then the flask was placed in a 105 $^\circ\text{C}$  silicone oil bath and stirred for 8 h. After the completion of the reaction, the mixture was cooled to room temperature and diluted in 200 mL of chloroform. And then washed by 1N NaOH solution and deionized water several times to eliminate the residual reactant. Then the product was dried over sodium sulfate, followed by filtration and drying under vacuum oven. Finally, a white fine powder with the yield of 81% was obtained. The reaction was illustrated in Scheme 1.

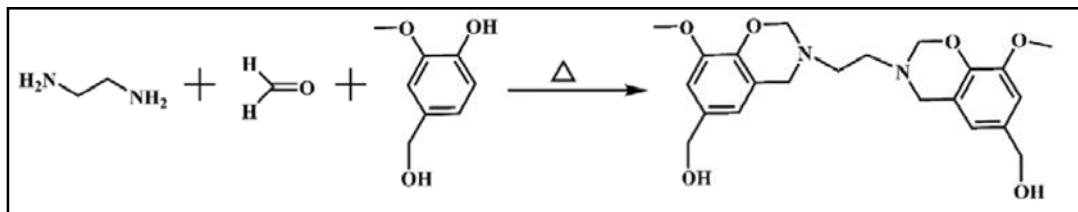


Scheme 1. Synthesis of bis-benzoxazine monomer G-e.

### Synthesis of vanillyl alcohol-based bis-benzoxazine precursor: Va-e

24.7 g vanillyl alcohol (0.16 mol), 4.8 g ethylenediamine (0.08 mol), 12.1 g paraformaldehyde (0.40 mol, 5.0 equiv.) and 150 mL 1,4-dioxane were introduced into a round-bottom 250 mL glass flask equipped with a nitrogen inlet, a condenser and a magnetic stirrer. Then the flask was placed in a 105 $^\circ\text{C}$  silicone oil bath and

stirred for 8 h. After the completion of the reaction, the mixture was cooled to room temperature and then diluted in 200 mL of chloroform. Then it was washed by 1N NaOH solution and deionized water several times to eliminate the residual reactant. Then the product was dried over sodium sulfate, followed by filtration and drying under vacuum oven. Finally, a light yellow powder with the yield of 78% was obtained. The reaction was illustrated in Scheme 2.

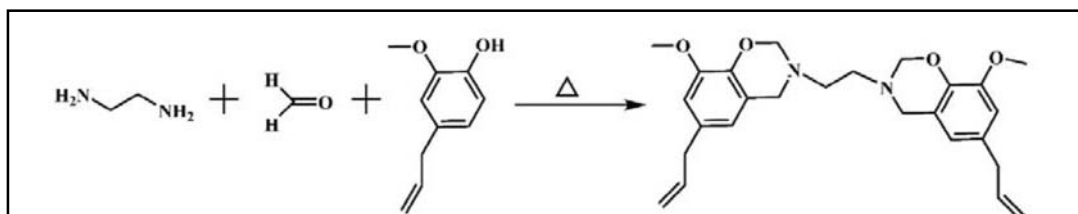


**Scheme 2.** Synthesis of bis-benzoxazine monomer Va-e.

**Synthesis of eugenol alcohol-based bis-benzoxazine precursor: E-e**

26.3 g eugenol (0.16 mol), 4.8 g ethylenediamine (0.08 mol), 12.1 g paraformaldehyde (0.40 mol, 5.0 equiv.) and 150 mL 1,4-dioxane were introduced into a round-bottom 250 mL glass flask equipped with a nitrogen inlet, a condenser and a magnetic stirrer. Then the flask was placed in a 105°C silicone oil bath and

stirred for 8 h. After the completion of the reaction, the mixture was cooled to room temperature and then diluted in 200 mL of chloroform. Then it was washed by 1N NaOH solution and deionized water several times to eliminate the residual reactant. Then the product was dried over sodium sulfate, followed by filtration and drying under vacuum oven. Finally, a white fine powder with the yield of 79% was obtained. The reaction was illustrated in Scheme 3.

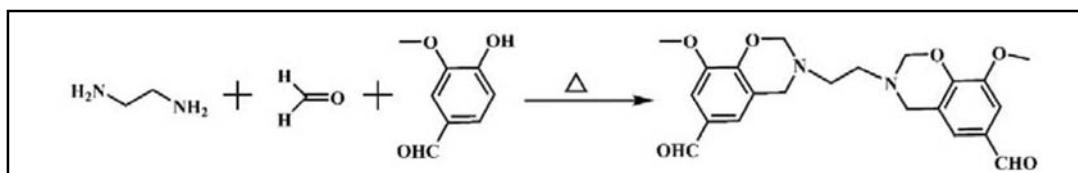


**Scheme 3.** Synthesis of bis-benzoxazine monomer E-e.

**Synthesis of vanillin-based bis-benzoxazine precursor: V-e**

Into a 250 mL round bottom flask equipped with a magnetic stirrer, 24.4 g vanillin (0.16 mol), 4.8 g ethylenediamine (0.08 mol), 12.1 g paraformaldehyde (0.40 mol, 5.0 equiv.) and 150 mL 1,4-dioxane were introduced into a round-bottom 250 mL glass flask equipped with a nitrogen inlet, a condenser and a magnetic stirrer. Then the flask was placed in a 105°C silicone oil

bath and stirred for 8 h. After the completion of the reaction, the mixture was cooled to room temperature and then diluted in 200 mL of chloroform. Then it was washed by 1N NaOH solution and deionized water several times to eliminate the residual reactant. Then the product was dried over sodium sulfate, followed by filtration and drying under vacuum oven. Finally, a light yellow powder with the yield of 68% was obtained. The reaction was illustrated in Scheme 4.



**Scheme 4.** Synthesis of bis-benzoxazine monomer V-e.

#### Crosslinking of the lignin-based benzoxazines

Each sample (G-e, Va-e, E-e and V-e) was placed in Teflon mold (10 × 10 × 1 mm) and then melted and polymerized. The polybenzoxazines were produced in an air-circulating oven according to the following heating schedule<sup>[26]</sup>: 180°C (2 h), 200°C (2 h), 220°C (2 h) and 240°C (2 h). Finally, the obtained polybenzoxazines were removed from the mold.

### RESULTS AND DISCUSSION

#### The chemical structures of the synthesized bis-benzoxazine monomers

The chemical structures of synthesized bis-benzoxazine monomers (G-e, Va-e, E-e and V-e) in this work were confirmed by the commonly used measuring methods, including FTIR, <sup>1</sup>H NMR and <sup>13</sup>C NMR. Figure 1 presented the FTIR spectra of guaiacol, G-e, vanillyl alcohol, Va-e, eugenol, E-e, vanillin and V-e, respectively. The FTIR spectra of guaiacol and the obtained benzoxazine compound G-e was shown in Figure 1a. From the spectrum of G-e, characteristic peaks of C-O-C were observed at 1052 cm<sup>-1</sup> and 1233 cm<sup>-1</sup>. Besides, the peak at 943 cm<sup>-1</sup> was assigned to the out-of-plane C-H stretching of oxazine ring, and the C-N-C bond of oxazine ring were appeared at 1362 cm<sup>-1</sup><sup>[27]</sup>. The fact that the FT-IR absorption band of O-H stretching vibration at nearby 3500 cm<sup>-1</sup> was observed for guaiacol and was non-existent for G-e indicates that the Mannich reaction completely proceeded. Meanwhile, for the spectrum of Va-e (Figure 1b), the peak at 942 cm<sup>-1</sup> was assigned to the out-of-plane C-H stretching of oxazine ring, and the peak at 1341 cm<sup>-1</sup> was assigned to the C-N-C bond of oxazine ring. In addition, the peaks at 1032 and 1233 cm<sup>-1</sup> represented the C-O-C stretching<sup>[27]</sup>.

Similarly, from Figure 1c and Figure 1d, the characteristic peaks of oxazine rings in the structure of E-e and V-e could be observed at 951, 1088, 1234, 1360 cm<sup>-1</sup> and 952, 1088, 1231, 1361 cm<sup>-1</sup>, respectively. Based on the above FTIR analysis, the structures of G-e, Va-e, E-e and V-e could be initially confirmed.

For further confirmation of the chemical structures, the NMR (<sup>1</sup>H NMR and <sup>13</sup>C NMR) spectra of synthesized benzoxazine monomer (G-e, Va-e, E-e and V-e) were shown in Figure 2. Correspondingly, all the characteristic peaks of the protons were identified. The peaks in all <sup>1</sup>H-NMR spectra at 4.82-5.08 ppm and 3.92-4.12 ppm were attributed to the protons of O-CH<sub>2</sub>-N and Ar-CH<sub>2</sub>-N, respectively<sup>[28]</sup>. Moreover, the peaks that appeared at 6.53-6.85 ppm (for G-e, Va-e and E-e) and 7.15-7.30 ppm (for V-e) were related to the protons of benzene ring. At the same time, the corresponding <sup>13</sup>C-NMR spectrum also confirmed the structure of synthesized benzoxazine monomer (G-e, Va-e, E-e and V-e). The two characteristic singles at 83.05-84.05 ppm and 49.99-50.11 ppm were the typical carbon resonances of N-CH<sub>2</sub>-O and N-CH<sub>2</sub>-Ar of the oxazine ring respectively<sup>[29]</sup>. In addition, the peaks of protons and carbons were all corresponding to the characteristic peaks of protons and carbons in target compounds (G-e, Va-e, E-e and V-e). All these results indicated that the desired compounds (G-e, Va-e, E-e and V-e) were synthesized successfully.

#### The polymerization behaviors of the synthesized monomers

In order to develop a greater knowledge of the curing process, the DSC curves of G-e, Va-e, E-e and V-e in the range of 50-350°C at a

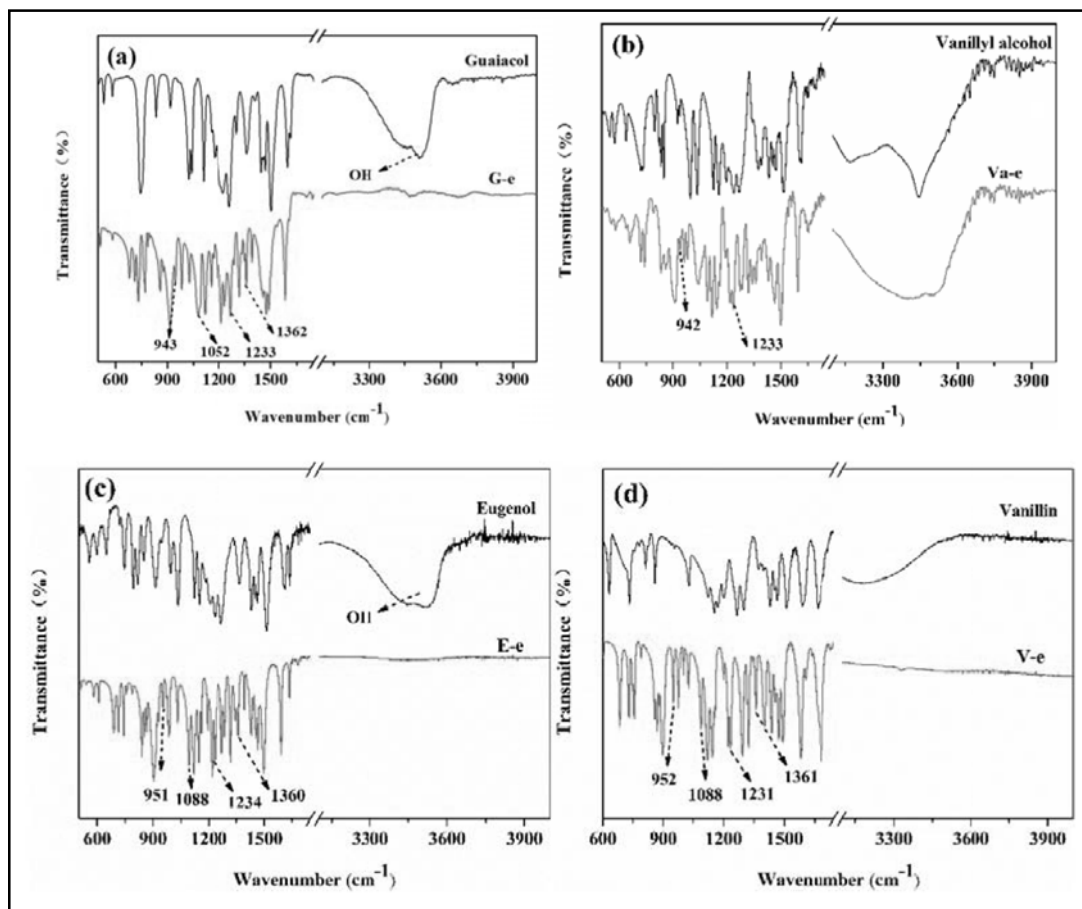


Fig. 1. The FTIR spectra of guaiacol, G-e, vanillyl alcohol, Va-e, eugenol, E-e, vanillin and V-e.

heating rate of 10°C/min were all shown in Figure 3. As shown, the endothermic peaks centered at 196, 170, 157 and 223°C should be the melting point of the synthesized benzoxazine monomers (G-e, Va-e, E-e and V-e). In addition, the exothermic peaks temperature were around 221, 202, 238 and 225°C for G-e, Va-e, E-e and V-e, respectively. Thus, it is obvious that the introduction of hydroxyl group into the phenol structure not

only decreases the melting point of the benzoxazine monomer, but also increases the curing activity of these benzoxazines. However, the allyl group in the structure of E-e slowed down the ring-opening polymerization reaction of oxazine rings due to being blocked at highly reactive para position of phenol. Likewise, paraposition blocked V-e also showed higher ring-opening polymerization temperature than G-e, although the introduction of electron-with

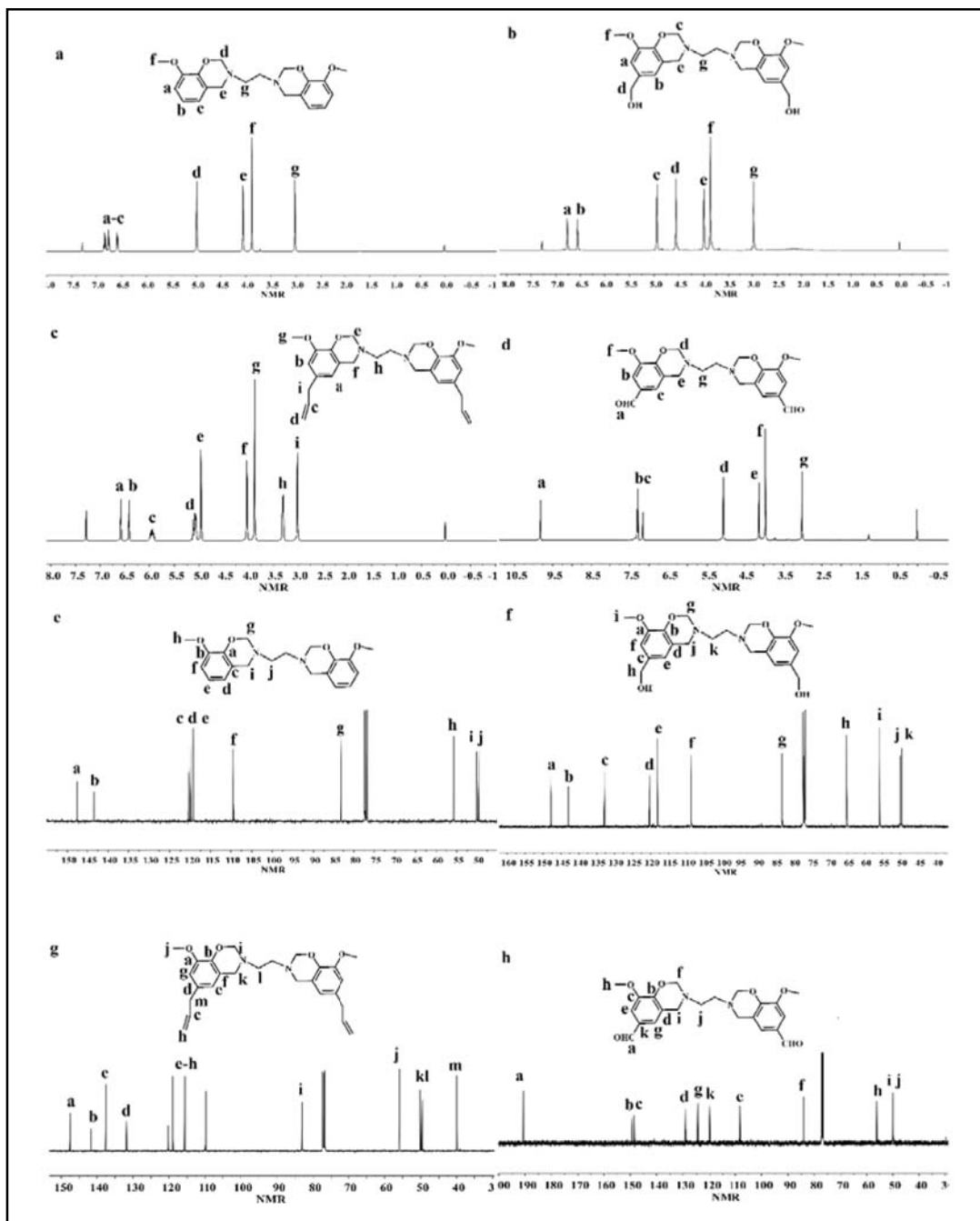


Fig. 2. The NMR spectra of G-e, Va-e, E-e and V-e.

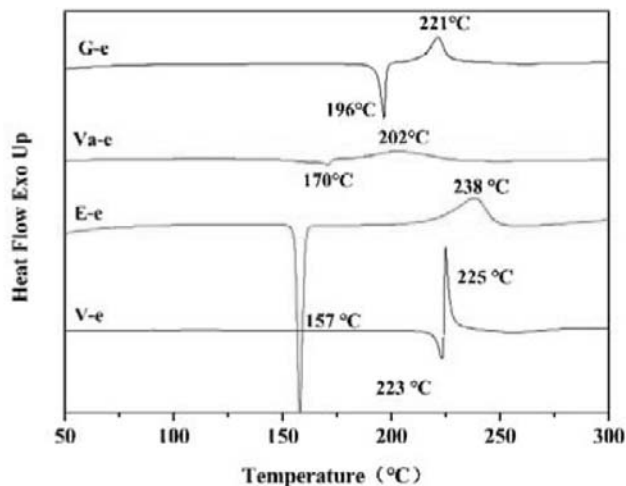


Fig. 3. The DSC curves of synthesized benzoxazine monomers (G-e, Va-e, E-e and V-e).

drawing aldehyde group into phenol structure could have accelerated the ring-opening polymerization reaction of oxazine rings.

To study the mechanism of curing reaction for benzoxazine monomer deeply, the multiple heating-rate method of dynamic mode was used to evaluate the polymerization reaction kinetic, which was performed on DSC. The non-isothermal DSC curing curves were all presented in Figure 4. As shown, the polymerization behaviors of synthesized benzoxazine monomers (G-e, Va-e, E-e and V-e) were both studied with DSC at heating rate of 5, 10, 15 and 20°C/min, with exothermic peaks appearing at 211, 221, 228, 232°C for G-e, 190, 202, 206, 211°C for Va-e, 228, 238, 244, 249°C for E-e and 215, 225, 229, 235°C for V-e, respectively. Furthermore, the synthesized benzoxazine monomers (G-e, Va-e, E-e and V-e) all showed a single exothermic peak, which was associated with the ring-opening polymerization of oxazine rings<sup>[30]</sup>.

In this work, the activation energy ( $E_a$ ) of the synthesized benzoxazine monomer is calculated by the Kissinger method, which is based on formula (1)<sup>[31,32]</sup>.

$$-\ln \frac{\beta}{T_p^2} = \frac{E_a}{RT_p} - \ln \frac{A'R}{E_a} \quad (1)$$

where  $\beta$  for the heating rate;  $T_p$  for the exothermic peak temperature of curing reaction in Kelvin;  $R$  for the gas constant;  $E_a$  for the activation energy. Based on the formula (1), the value of reaction activation energy ( $E_a$ ) for G-e system was calculated to be 124.42 kJ/mol (Figure 5). It's worth noting that the  $E_a$  of Va-e system in curing reaction were lower than G-e system, showing 116.23 kJ/mol. For the Va-e system, the hydroxyl structure play a positive role in promoting oxazine ring opening of benzoxazine precursors and then led to the decreased  $E_a$ <sup>[33]</sup>. At the same time, E-e and V-e systems exhibited higher  $E_a$  than G-e system, suggesting a lower ring-opening



polymerization activity, which corresponded with the exothermic peaks temperature discussed above.

Besides, the rate of polymerisation of G-e, Va-e, E-e and V-e were measured by the rheological analyze. And their viscosities

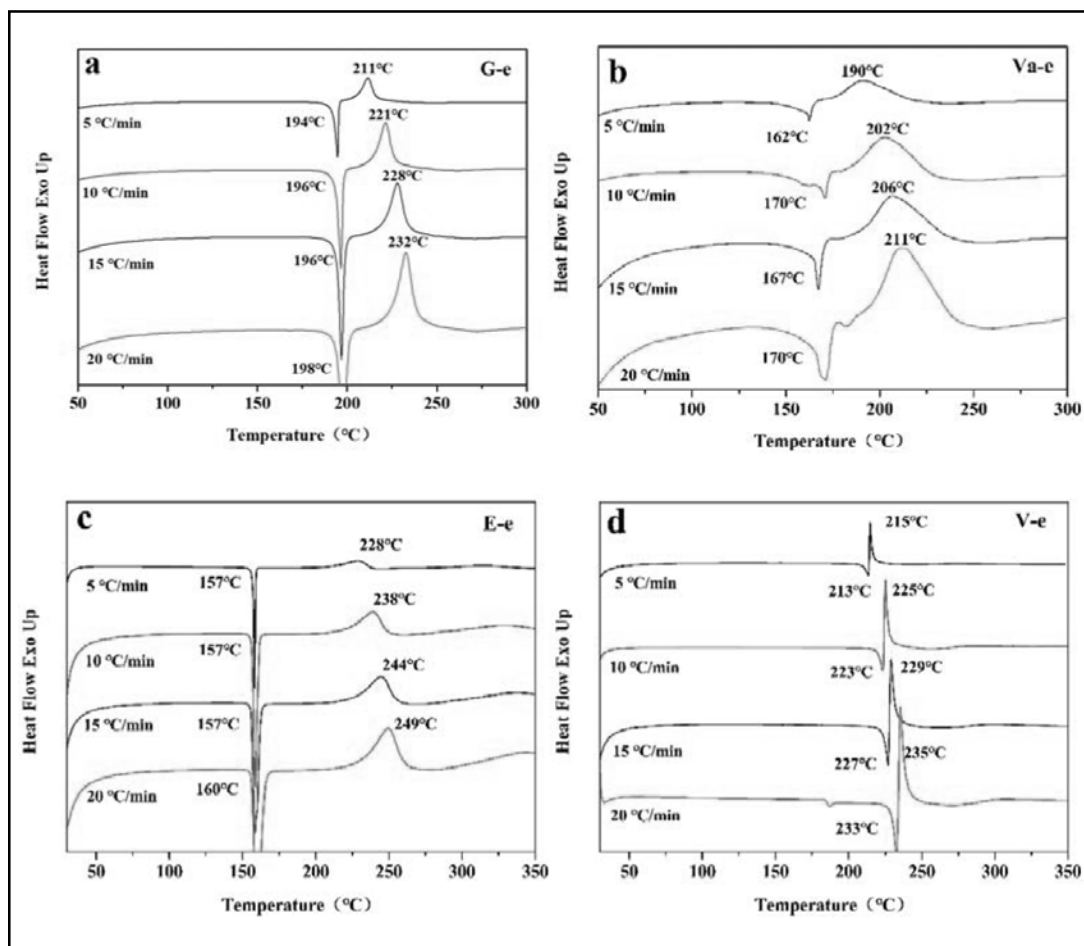


Fig. 4. The DSC curves of synthesized benzoxazine monomers (G-e, Va-e, E-e and V-e).

as function of heating time were shown in Figure 6. The gelation points of G-e, Va-e, E-e and V-e at 200°C were 13.4 min, 6.7 min, 55.6 min and 32.1 min, respectively. Obviously, these results corresponded with the activation energy ( $E_a$ ) discussed above.

### The thermal stability of the bio-based polybenzoxazines

In this work, the thermal degradation behavior of the bio-based polybenzoxazines cured from G-e, Va-e, E-e and V-e was studied through

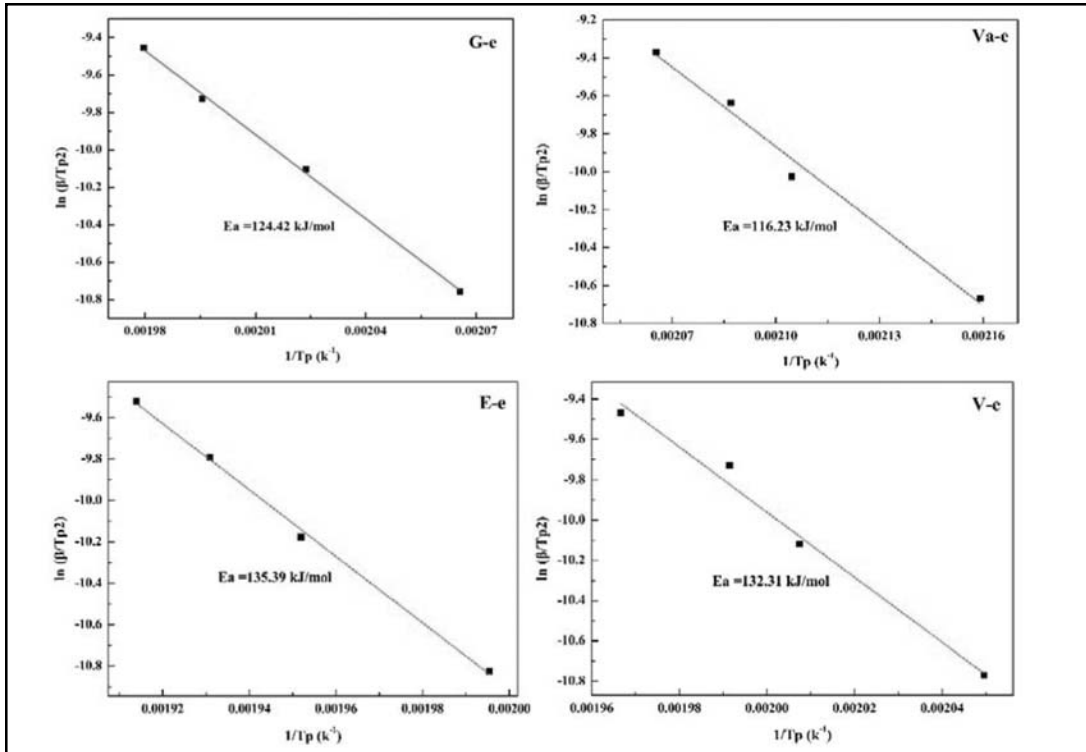


Fig. 5. The relationship between  $\ln(\beta/T_p^2)$  and  $1/T_p$  for G-e, Va-e, E-e and V-e.

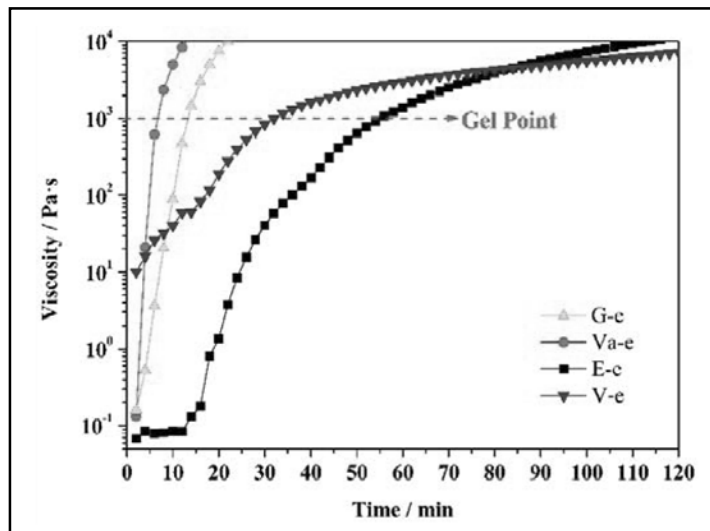


Fig. 6. Isothermal rheology monitoring of G-e, Va-e, E-e and V-e at 210°C

TGA between 50 and 800°C under the atmosphere of nitrogen, and the detail data were both shown in Figure 7. As shown, it clearly that all the polybenzoxazines cured from G-e, Va-e, E-e and V-e exhibited well thermal stability. They were stable below 300°C under the atmosphere of nitrogen. Furthermore, poly (G-e) possessed the best thermal stability, showing 5% weight loss temperatures ( $T_{d5\%}$ ) and char yield at 800°C ( $R_{800}$ ) of 339°C and 51.2%, respectively, which is due to the high crosslink density generated by highly reactive para position of G-e. poly(E-e) showed slightly lower  $T_{d5\%}$  of 336°C than poly(G-e) in spite of para position blocked structure, because the radical polymerization of allyl existed during the curing process of E-e. In addition, the hydroxyl and aldehyde group introduced in the structure of polybenzoxazines were more easy to be

decomposed. Similar results were also reported previously<sup>[34]</sup>.

## CONCLUSIONS

In this work, four novel bio-based benzoxazine resins (G-e, Va-e, E-e and V-e) were synthesized from bio-based monomers (guaiacol, vanillyl alcohol, eugenol and vanillin) and successfully polymerized to produce the corresponding polybenzoxazines. DSC results showed that the melting point, onset curing temperature and the activation energy ( $E_a$ ) of Va-e was lower than that of G-e, which was considered to be caused by the introduction of hydroxyl group into the structure of benzoxazine. Meanwhile, being blocked at highly reactive para position of phenol resulted in lower ring-opening polymerization activity of E-e and V-e than

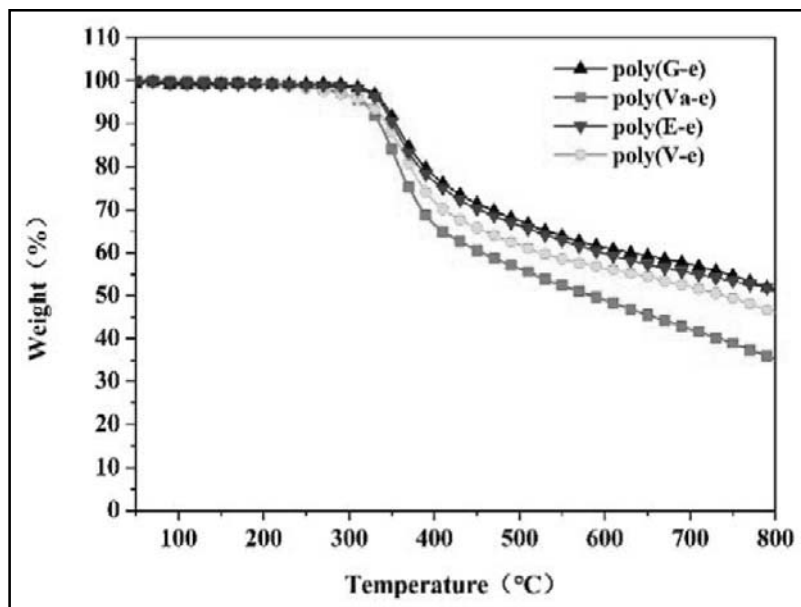


Fig. 7. TGA curves of the different polybenzoxazine resins under nitrogen.

G-e. In addition, the TGA results demonstrated that the thermal stability of polybenzoxazines could be weakened due to the introduction of hydroxyl group and aldehyde group.

### ACKNOWLEDGMENTS

The authors are grateful for the financial support from Chengde high-tech industrial development zone “Chengde co-creation Space Project” CGX2018KMP0004.

### REFERENCES

1. K. Zhang, Q. Zhuang, X. Liu, G. Yang, R. Cai, Z. Han, *Macromolecules* 46 (2013) 2696-2704.
2. L. Zhang, Y. Yang, Y. Chen, H. Lu, *European Polymer Journal* 93 (2017) 284-293.
3. L. Dumas, L. Bonnaud, M. Olivier, M. Poorteman, P. Dubois, *Green Chemistry* (2016).
4. P. Froimowicz, K. Zhang, H. Ishida, *Chemistry* 22 (2016) 2691-2707.
5. K. Zhang, P. Froimowicz, L. Han, H. Ishida, *Journal of Polymer Science Part A Polymer Chemistry* 54 (2016) 3635-3642.
6. K. Zhang, H. Ishida, *Polymer Chemistry* 6 (2015) 2541-2550.
7. P. Froimowicz, R.A. C, L. Han, H. Ishida, *Chemsuschem* 9 (2016) 1898-1898.
8. L. Han, K. Zhang, H. Ishida, P. Froimowicz, *Macromolecular Chemistry & Physics* 218 (2017) 1600562.
9. J.M. Raquez, M. Deléglise, M.F. Lacrampe, P. Krawczak, *Progress in Polymer Science* 35 (2010) 487-509.
10. A. R, C. S, D. G, B. B, P. JP, Biobased thermosetting epoxy: present and future, *Chemical Reviews* 114 (2014) 1082-1115.
11. M. Fache, R. Auvergne, B. Boutevin, S. Caillol, *European Polymer Journal* 67 (2015) 527-538.
12. A. Yamaguchi, N. Mimura, M. Shirai, O. Sato, *Journal of the Japan Petroleum Institute* 59 (2016) 155-159.
13. V.K. Thakur, M.K. Thakur, R.K. Gupta, *International Journal of Biological Macromolecules* 61 (2013) 121-126.
14. M.K. Thakur, A.K. Rana, V.K. Thakur, *Lignocellulosic Polymer Composites: A Brief Overview*, John Wiley & Sons, Inc., 2014.
15. C. Asada, S. Basnet, M. Otsuka, C. Sasaki, Y. Nakamura, *International Journal of Biological Macromolecules* 74 (2015) 413-419.
16. H. S, L. X, L. Y, *ChemInform* 45 (2014) no-no.
17. S. Hu, Y. Li, *Bioresour Technol* 161 (2014) 410-415.
18. I. Delidovich, P.J. Hausoul, L. Deng, R. Pfützenreuter, M. Rose, R. Palkovits, *Chemical Reviews* 116 (2016) 1540.
19. M. Brebu, C. Vasile, *Cellulose Chemistry & Technology* 44 (2010) 353-363.
20. A. Llevot, E. Grau, S. Carlotti, S. Grelier, H. Cramail, *Macromolecular rapid communications* 37 (2016) 9-28.
21. G.M. Rashid, M.J. Duran-Pena, R. Rahmanpour, D. Sapsford, T.D. Bugg, *Journal of Applied Microbiology* 123 (2017).
22. G.J. Abarro, J. Podschun, L.J. Diaz, S. Ohashi, B. Saake, R. Lehnen, H. Ishida, *Rsc Advances* 6 (2016).
23. G.A. Phalak, D.M. Patil, S.T. Mhaske, *European Polymer Journal* 88 (2016).
24. P. Thirukumar, A. Shakila, S. Muthusamy, *Rsc Advances* 4 (2014) 7959.
25. N.K. Sini, J. Bijwe, I.K. Varma, *Polymer Degradation & Stability* 109 (2014) 270-277.
26. A. Trejo-Machin, P. Verge, L. Puchot, R. Quintana, *Green Chemistry* (2017).

27. T. Agag, S. Geiger, S.M. Alhassan, S. Qutubuddin, H. Ishida, *Macromolecules* 43 (2010) 7122-7127.
28. Y. Cheng, J. Yang, Y. Jin, D. Deng, F. Xiao, *Macromolecules* 45 (2012) 4085-4091.
29. X. Liu, R. Zhang, T. Li, P. Zhu, Q. Zhuang, *ACS Sustainable Chemistry & Engineering* (2017).
30. L. Dumas, L. Bonnaud, M. Olivier, M. Poorteman, P. Dubois, *European Polymer Journal* 75 (2016) 486-494.
31. R. Andreu, J.A. Reina, J.C. Ronda, *Journal of Polymer Science Part A Polymer Chemistry* 46 (2010) 6091-6101.
32. B. Kiskan, B. Koz, Y. Yagci, *Journal of Polymer Science Part A Polymer Chemistry* 47 (2010) 6955-6961.
33. W. Men, Z. Lu, Z. Zhan, *Journal of Applied Polymer Science* 109 (2010) 2219-2223.
34. D.K. Shen, S. Gu, *Bioresource Technology* 100 (2009) 6496-6504.

Received: 10.01.2019

Accepted: 11.03.2019